Robust and Intelligent Bearing Estimation

John P. Claassen, Monitoring Technologies Department, Sandia National Laboratories

Sponsored by the U. S. Department of Energy
Office of Nonproliferation and National Security
Office of Research and Development
Contract No. DE-AC04-94AL8500

Abstract

As the monitoring thresholds of global and regional networks are lowered, bearing estimates become more important to the processes which associate (sparse) detections and which locate events. Current methods of estimating bearings from observations by 3-component stations and arrays lack both accuracy and precision*. Methods are required which will develop all the precision inherently available in the arrival, determine the measurability of the arrival, provide better estimates of the bias induced by the medium, permit estimates at lower SNRs, and provide physical insight into the effects of the medium on the estimates. Initial efforts have focused on 3-component stations since the precision is poorest there.

An intelligent estimation process for 3-component stations has been developed and explored. The method, called SEE for Search, Estimate, and Evaluate, adaptively exploits all the inherent information in the arrival at every step of the process to achieve optimal results. In particular, the approach uses a consistent and robust mathematical framework to define the optimal time-frequency windows on which to make estimates, to make the bearing estimates themselves, and to withdraw metrics helpful in choosing the best estimate(s) or admitting that the bearing is immeasurable. The approach is conceptually superior to current methods, particularly those which rely on real valued signals.

The approach features a quadrature digital filter bank whose individual filters are based on Slepian wavelets with a slight but important modification. The quadrature signal components are used to construct a series of rectangular observation matrices each centered on a given time-frequency interval. The degree of polarization, the linearity of the particle motion, the degree to which the eigen energy is concentrated, and a pseudo SNR are estimated from each observation matrix. Bearings are estimated from a concatenated set of time-frequency intervals having polarization properties most likely to produce accurate estimates. Among the available estimates, the choice or construction of the best estimate is currently guided by a simple information theoretic principle, although continued investigations are likely to uncover alternative methods of statistically combining and selecting estimates.

The method has been evaluated to a considerable extent in a seismically active region and has demonstrated remarkable utility by providing not only the best estimates possible but also insight into the physical processes affecting the estimates. It has been shown, for example, that the best frequency at which to make an estimate seldom corresponds to the frequency having the best detection SNR and sometimes the best time interval is not at the onset of the signal. The method is capable of measuring bearing dispersion, thereby withdrawing the bearing bias as a function of frequency. The lowest measurable frequency in the dispersion pattern is often a near error free bearing. These latter features should be helpful in calibrating the stations for frequency dependent biases induced by the earth. Future efforts will enhance the SEE algorithm and will also evaluate it using larger station data sets.

Key Words: Bearing Estimation, Associations, Location

*Accuracy is here defined as the precision of the measurement plus the (mean) bias. Precision is regarded as the rms fluctuation in the estimates.

DISCLAIMER

DISCLAIMER

Portions of this document may be illegible electronic image products. Images are produced from the best available original document.

Objectives

As the monitoring thresholds of global and regional networks are lowered, bearing estimates become more important to the processes which associate (sparse) detections and which locate events. Current methods of estimating bearings from observations by 3-component stations and arrays lack both accuracy and precision [1][2]. Methods are required which will develop all the precision inherently available in the arrival, determine the measurability of the arrival, provide better estimates of the bias induced by the medium, permit estimates at lower SNRs, determine the precision of the estimate, and provide physical insight into the effects of the medium on the estimates.

This work specifically focused on developing an adaptive intelligent method of estimating bearings from 3-component data and on evaluating the approach on a limited but challenging set of regional events observed in an active tectonic region. The method, called SEE for Search, Estimate, and Evaluate, seeks to exploit all the inherent information in the observations to achieve near optimal results at every step of the process.

Research Accomplished

Overview of the Method

Consistent mathematical and statistical frameworks were used to develop a robust process for estimating bearings from 3-c station data. The process, depicted in Figure 1, searches for those time-spectral windows having optimal polarization properties on which to make bearing estimates, makes estimates on intervals having the best polarization properties, and withdraws metrics helpful in choosing the best estimate(s) or discarding all estimates when none is possible. The process is based on the following assumptions: 1) not all frequencies or time intervals will be equally effective in producing measurable bearings, 2) only those time-frequency windows having good polarization properties will result in usable estimates, 3) the estimates themselves may be frequency dependent, i.e., frequency dependent refraction or scattering, and 4) those estimates having the largest degrees of freedom will experience the greatest variance reduction and therefore are the best estimates to combine for a refined estimate which may include bias corrections.

Implementation

The filter bank shown in Figure 1 is based on Slepian wavelets [3] and was used to spectrally decompose the 3-c signals into quadrature signals whose center frequencies were logarithmically spaced and whose bandpasses overlap by approximately 50%. Individual filters in the bank were characterized by a constant time-bandwidth product. In order to minimize the bandpass leakage, the Slepian wavelet coefficients were weighted by a Hanning function. The bandpass characteristic of the filter bank is illustrated in Figure 2.

At a given center frequency f_c and a given sample m_o, complex valued signals with bandwidth f_w were used to prepare a rectangular observation matrix of the form

$$\boldsymbol{R}(f_c, f_w, m_o) = \left[s_x(f_c, f_w, m_o)\ s_y(f_c, f_w, m_o)\ s_z(f_c, f_w, m_o) \right]$$

where $s_i(f_c f_w m_o)$ is a vector of complex valued signal samples observed on the ith axis of the seismometer and centered about sample m_o. The singular values and right singular vectors of $\boldsymbol{R}$ may be used to define various "instantaneous" polarization properties [4][5][6] of the 3-c signal segment centered about sample m_o. Several of the useful polarization properties used in this work are illustrated by the spectrograms of Figures 3 and 4 where polarization measures are shown relative to the P wave signal on the z axis. The graph of Figure 3 specifically illustrates that the degree of polarization (DOP) can localize the more favorable time and frequency intervals on which to make bearing estimates. The graph of Figure 4 indicates that the linearly polarized regions can provide additional information on selecting those intervals. In both cases polarization measures nearing one are considered strong responses. In interpreting these spectrograms, the reader is cautioned that a polarization response can occur before the actual onset of the signal since the quadrature filters are non-causal. These illustrations demonstrate that an assortment of measures is helpful in searching for those time-frequency windows having strong polarization properties. Bearing estimates are formed on those intervals having the best set of properties.

The importance of the polarization measures in selecting the proper frequency-time intervals on which to make bearing estimates can, perhaps, be best illustrated by examining a coherency based signal to noise ratio (SNR), an example of which appears in the graph of Figure 5. It is known that the best detection SNR occurs near 1.5 Hz for this arrival. Yet, the graph of Figure 5 suggests that not only should 1.5 Hz be considered for bearing estimates but that lower frequencies should also be considered. As will be shown, the bearing estimates at the lower frequencies are actually more accurate than the estimates at the higher frequencies (See Figure 8).

Bearing estimates can be formed in a number of ways as discussed by Walck and Chael [7]. In this work the bearing and apparent incident angle were simply based on the principal singular vector of a rectangular observation matrix associated with a selected window. This approach results in a bearing estimate for each of the selected time-frequency windows. Among all the available estimates, the best estimates are currently chosen on the basis of an information theoretic measure which reflects the degree of variance reduction in the estimate. This evaluation/selection measure states that the variance is reduced by the product of the SNR and the time-bandwidth product (TB) associated with the observation. To form this evaluation measure, the SNR is estimated from the (polarized) coherence properties of the selected window and the TB product is based on the duration of the window and the bandwidth of the filter. In this work the SNR*TB product will be called the effective degrees of freedom (DOF). Only those estimates whose effective DOF exceed a given threshold are accepted as valid estimates. A consequence of the current acceptance process is that multiple or no answers are provided. Eventually, the shortcoming of multiple answers will be overcome, probably with the use of an approach described below.

Application of the Method

The polarization based bearing estimator was applied to a reasonably large set of regional P arrivals arising from events located in the western US and observed at a high frequency station located near Pinedale, Wyoming*. The arrivals were extracted from the S-3 seismometer channel which had been electronically altered to provide an acceleration output having a nominal 0.5 to 80 Hz bandpass. The bearing estimates were restricted to the central frequencies associated with the filter bank (0.5 to 15 Hz). The locations of the events contributing to an initial evaluation of the SEE algorithm appear in the map of Figure 6.

Bearing error estimates of a select set of events, as inferred from the NEIC locations, are presented here to illustrate the efficacy of the SEE approach. The errors are compared with the error associated with a conventional broadband estimator whose solution is based on the initial arrival and the principal eigenvector of a real valued covariance matrix. Only those estimates having effective DOF above a threshold were accepted and plotted. For most of the error plots a composite polarization indicator reflecting a mixture of polarization measures appears above the bearing error plot to make evident the SEE rationale. The bearing errors are drawn over the measurable time-interval as inferred from the polarization properties. The frequency, at which the estimate was made, is symbol and color encoded in accord with a key appearing to the right. The key also provides the effective DOF (SNRTB) and the actual bearing estimate (PHI) associated with each measurable SEE window.

The graph of Figure 7 illustrates that the SEE approach can produce nearly correct estimates when the conventional approach fails. This arrival was produced by a quarry shot in eastern Wyoming at a range of 3.4 degrees. Here good estimates appear not only at the onset but also over interior portions of the P arrival. The estimate having the largest DOF (43.4) was able to produce the "true" bearing. The broadband SNR for this arrival is apparently poor as implied by a comparison of signal and noise amplitudes; however, the SEE approach was capable of identifying spectral components and time intervals having usable polarized states.

When the estimator was applied to an arrival emanating from a magnitude 5.8 earthquake in southern Utah at a range of 6.4 degrees, an interesting bearing dispersion characteristic emerged. As the error graph of Figure 8 indicates, the initial arrival exhibits bearings which move with frequency to the left of the event as observed from the recording station. The best bearing estimate occurs at the lowest frequency. Lateral refraction apparently causes bearing errors as large as 20 degrees at a frequency of 2.35 Hz. Furthermore, the conventional broadband estimate appears to be a frequency weighted average of the bearings associated with the different frequencies. Further evidence of refraction in Utah is documented by the bearing estimates for an earthquake occurring in northern Utah at a range of 3.1 degrees.

*The Pinedale database and event truth were provided by Dorthe Carr, SNL

Here, the estimate for the conventional broadband approach also appears to be a frequency weighted average of the frequency dependent bearings.

This dispersion characteristic was, in fact, observable in the 3-c signals associated with earthquakes all along the Wasatch mountains which run diagonally from northeastern Utah to southwestern Utah. A very conceivable explanation for the dispersion is the lateral variation in propagational velocities appearing across Utah as illustrated by the graph of Figure 10. This graph portrays the small changes in P velocity at a depth of 100 km as reported by Dueker [8] of the University of Colorado. The color encoded scale covers velocity gradients of ±5 % about 8.23 km/sec. These small velocity gradients undoubtedly extrapolate to the uppermost mantle and lower crust and therefore influence regional P arrivals also. The propagational velocity beneath the warmer Wasatch range is lower than the cooler Colorado plateau to the east. It is this velocity contrast which is thought to cause frequency dependent refraction of the P arrival for events arising along this mountain range.

It appears that significant bearing dispersion can also occur over local distances as illustrated by the bearing errors shown in Figure 11. Here an event 1/2 degrees east of the Pinedale station produced a complicated bearing pattern which initially moves approximately 15 degrees to the left of the bearing estimated at the lowest frequency and then wraps back to the right at higher frequencies. Confirmation of the bearing dispersion to the left is provided by the estimates associated with a second P arrival which is thought to be a shallow one. The wrapping of the estimates back to the right is not substantiated by the second arrival. The dispersion to the left is strongly confirmed by several high confidence estimates associated with the first arrival; whereas, the dispersion to the right cannot be confirmed with high confidence estimates.

Bearing dispersion was frequently evident in the estimates for many of the events. Some dispersion patterns moved to the left and some to the right of the actual event bearing with increasing frequency. Others appear to be scattered about a biased bearing. Some of the patterns appear to be associated with the known tectonics in this area. For example, events north and west of the Yellowstone hot spot are strongly refracted to the right. Some of complicated bearing patterns from southern Colorado may have been influenced by the crustal and upper mantle discontinuity along the Wyoming-Colorado border where island arcs are thought to have collided with the North American plate in an earlier geological era [8] and by the warm spot beneath the Sawatch Range. These observations appear to contradict the usual hypothesis where the deviations are attributed to scattering beneath the receiver or source. To observe these orderly dispersions it is important to accept bearing estimates having a sufficient number of effective degrees of freedom, in other words, when the statistical confidence is sufficiently high. Other careful processing considerations, too numerous to list here, are also required to make the bearing progression, when it occurs, clearly apparent.

Other attractive features of the SEE approach became evident during the investigation. The estimates of Figure 12 show that the best bearing may not always be available at the onset of the arrival. This arrival arose from a quarry blast in eastern Wyoming. The bearing plot demonstrates that the searching method can find frequency-time intervals which yield good estimates under high background and coda noise conditions. Although an assortment of bearings passed the acceptance criterion, the bearing having the highest degrees of freedom gave the best estimate. The final choice of bearing may have to be coupled with the location process to discard inconsistent bearings.

Another attractive feature of the SEE process is that the search for measurable time-frequency windows may at times indicate that there are no windows in which one can reasonably produce estimates with high confidence. This feature is illustrated by the composite polarization indicator of Figure 13 where attempts to find a sufficiently "long and strong" window failed. This arrival arose from an earthquake located in northern Utah at a range of 3.6 degrees. The signal exhibits a weak polarization property almost everywhere except for a very short interval centered about 1.72 Hz. But even there, the available effective DOF (11.9) failed to meet a reasonable acceptance threshold. Under these circumstances, the path structure or the distributive nature of the source may be so complicate that a coherent/polarized outcome cannot be constructed from the received signals. Because coherency measures are inherently embedded in the SEE process, a strong basis for discarding an estimate can be constructed.

Largely favorable outcomes have been reported to this point. It must be stated that for some events a strong physical or statistical basis for accepting the estimates cannot be found. In this research phase some of the confusion in accepting the outcomes may occur because the ground truth for some of the events is inaccurate. But in other cases the structural properties of the path may cause significant loss in polarization content or give rise to a large scatter of bearings. In the case of quarry blasts, the slowly emergent signal is composed of a mixture of weak temporal arrivals which ap-

pear to destroy the coherence required to make an estimate. On the other hand for measurable events SEE can provide additional insight at differing time-frequency windows in comparison to conventional approaches producing a single estimate.

Conclusions and Recommendations

The robust and intelligent bearing estimator, SEE, has demonstrated remarkable utility by providing not only the best possible estimates but also insight into the physical and statistical processes which affect the individual estimates. SEE has demonstrated that it can be hazardous to arbitrarily choose a time interval or a band of frequencies on which to make an estimate. In doing so the most useful polarized energy may be missed entirely or a weakly polarized signal may be accepted. It is essential to *Search* for the appropriate time-frequency windows having good polarized content before making an estimate. Furthermore, it is more important to use a SNR based on polarized coherency rather than on conventional pre-event noise measures to define a given window. It has also been shown that it can be inappropriate to make broadband estimates, for it may result in a frequency weighted average of a set of dispersed bearings, particularly in active tectonic areas. Instead, *Estimates* should be formed on narrow bands and hopefully long time intervals having strong polarization to achieve all the precision inherently available. The use of an *Evaluation* parameter based on the effective degrees of freedom is a viable approach for accepting the better estimates. Among those accepted estimates, one may have to apply a frequency dependent bias correction to account for the dispersion induced by the medium. The application of a frequency dependent bias to the individual estimate is probably the key to producing an estimate having superior accuracy.

Future efforts will consider applying SEE to other types of polarized arrivals and perhaps to their codas. Additional efforts must also address the need for producing one final estimate for the association and location processes. It appears that the lowest usable frequency having an acceptable number of degrees of freedom may be the key to providing the association process with the best initial bearing estimate. The application of a frequency dependent bias to a collection of the individual high confidence estimates and averaging the corrected estimates may provide the location process with the best possible bearing. These conjectures and others must be tested on a larger set of events in the future.

References

[1] Alewine, R. W., The Role of Arrays in Global Monitoring Systems, *Proc. of the GERESS Symposium*, Waldkirchen, pp. 2224, 1992

[2] Koch, K., and U. Kradolfer, Investigation of Azimuth Residuals Observed at Stations of the GSETT-3 Alpha Network, *Bull. of the Seismological Soc. of America*, Vol. 87, No. 6, pp. 1576-1597, December 1997

[3] Lilly, J. M. and J. Park, Multiwavelet Spectral and Polarization Analysis of Seismic Records, *Geophysical Journal International*, Vol. 122, pp. 1001-1021, 1995

[4] Samson, J. C., The Spectral Matrix, Eigenvalues, and Principal Components in the Analysis of Multi-channel Geophysical Data, *Ann. Geophysicae*, Vol. 1, No. 2, pp. 115-119, April 1983

[5] Vidale, J. E., Complex Polarization Analysis of Particle Motion, *Bull. of the Seismological Soc. of America*, Vol. 76, No. 5., pp. 1393-1405, October 1986

[6] Jurkevics, A., Polarization Analysis of Three-Component Array Data, *Bull. of the Seismological Soc. of America*, 78, No. 5., pp. 1725-1743, October 1988

[7] Walck, M. C. and E. P. Chael, Optimal Backazimuth Estimation for Three-Component Recordings of Regional Seismic Events, *Bull. of the Seismological Soc. of America*, Vol. 81, No. 2, pp. 643-666, April 1991

[8] Dueker, K. M., Personal Communication, University of Colorado, 1998

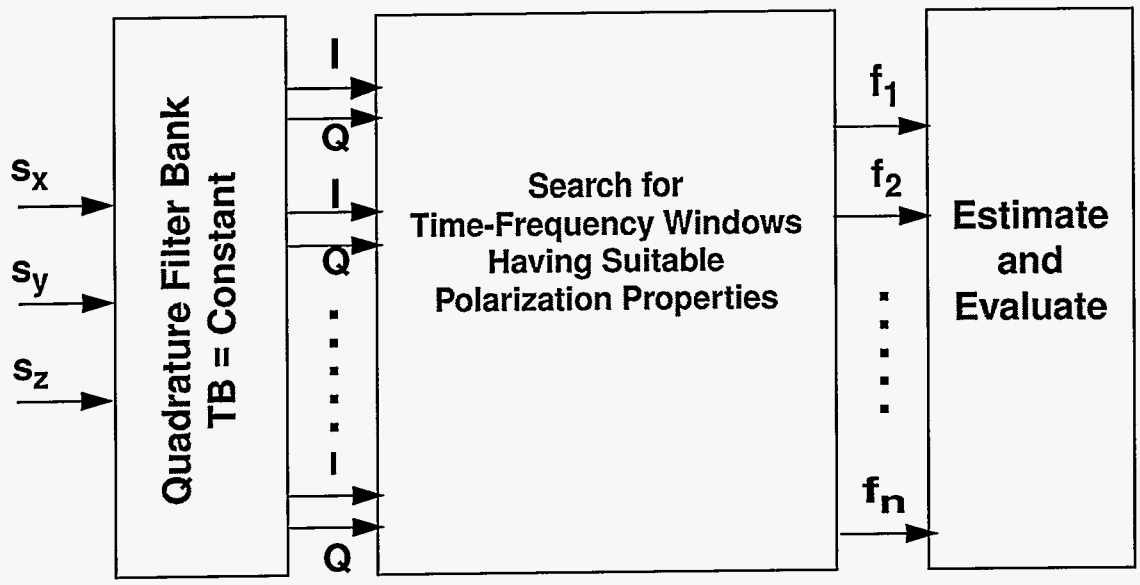

Figure 1. Block Diagram of the SEE Bearing Estimation Process

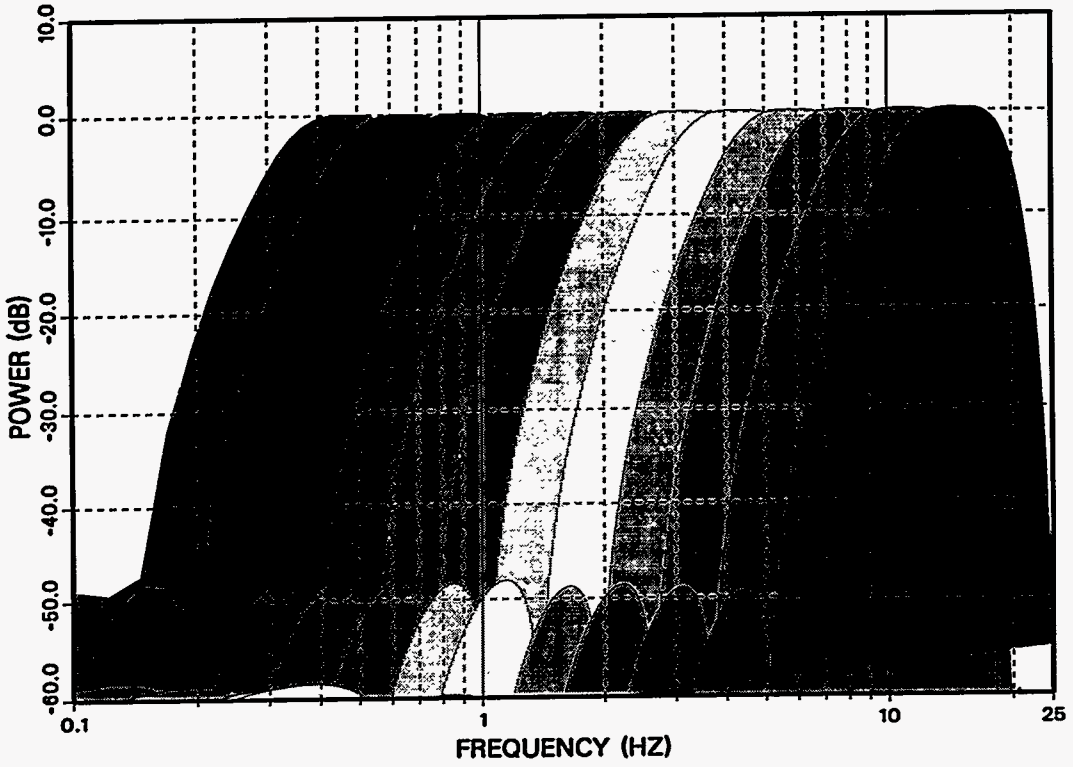

Figure 2. The Bandpass Characteristic of the Quadrature Filter Bank

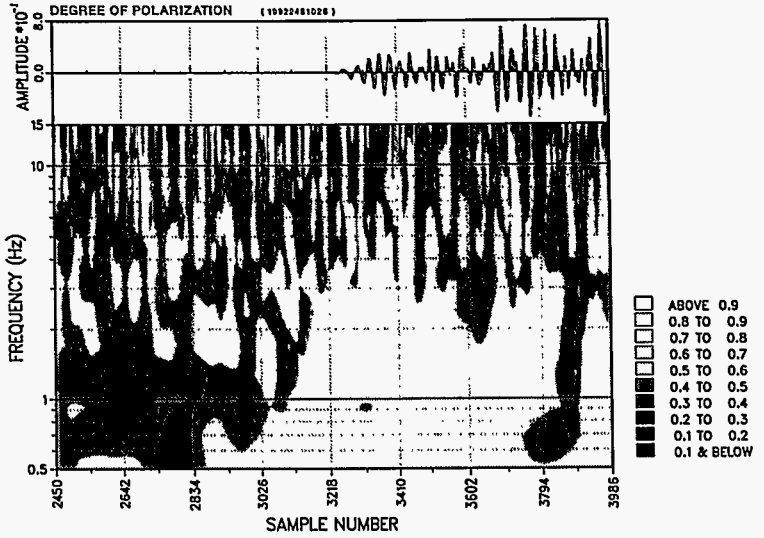

Figure 3. The Degree of Polarization (DOP) Localizes Favorable Time and Frequency Intervals for Estimation

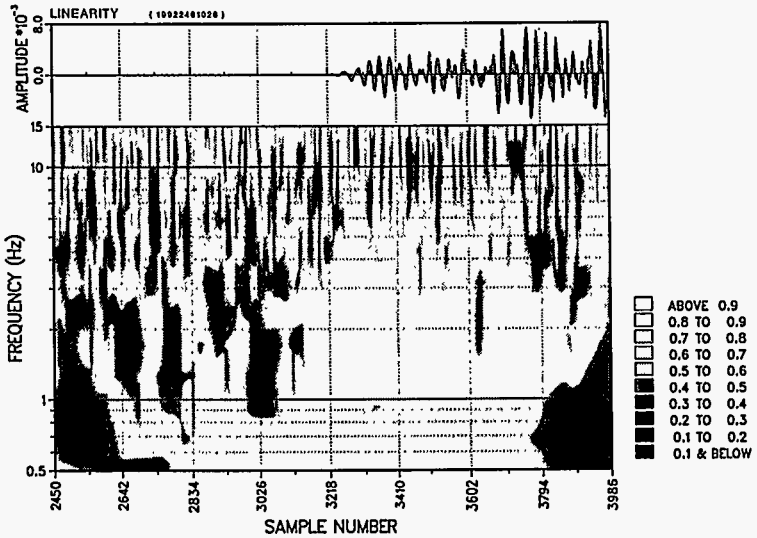

Figure 4. The Degree of Linear Polarization Provides Additional Localization Information

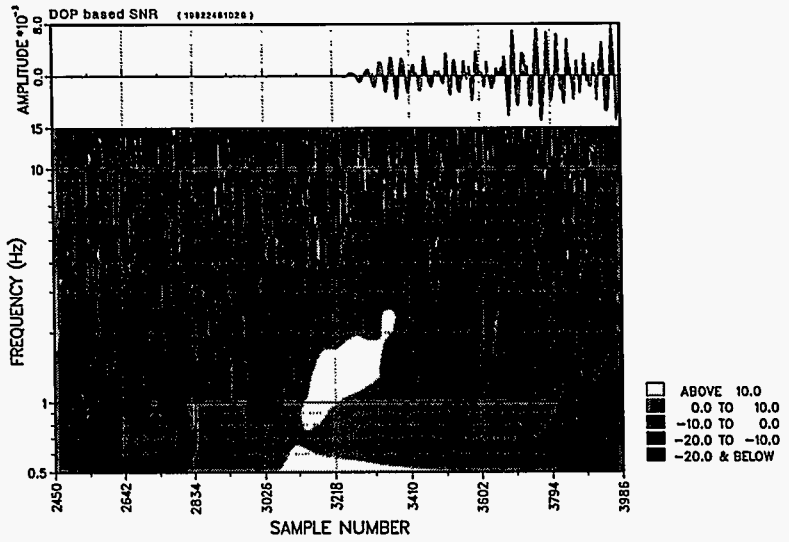

Figure 5. Coherency Based SNR Shows that the Best Polarized SNR May Differ with the Best Detection SNR

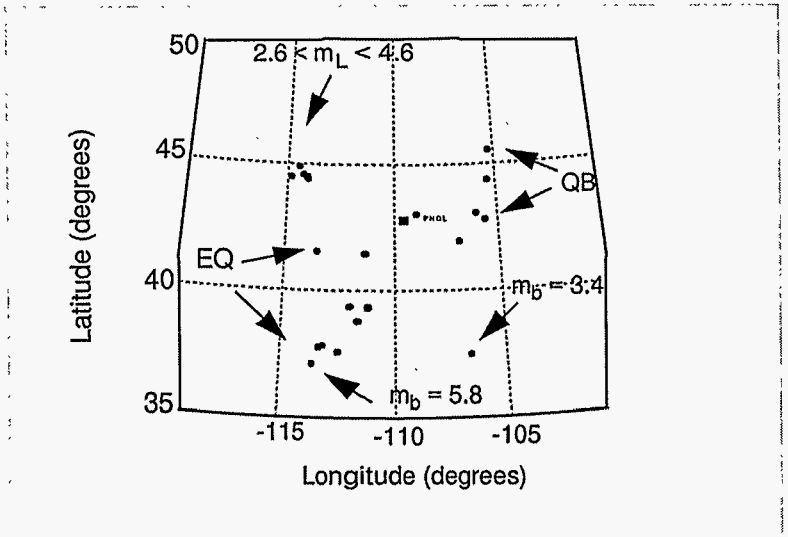

Figure 6. Locations of the Events Contributing to an Evaluation of the SEE Algorithm

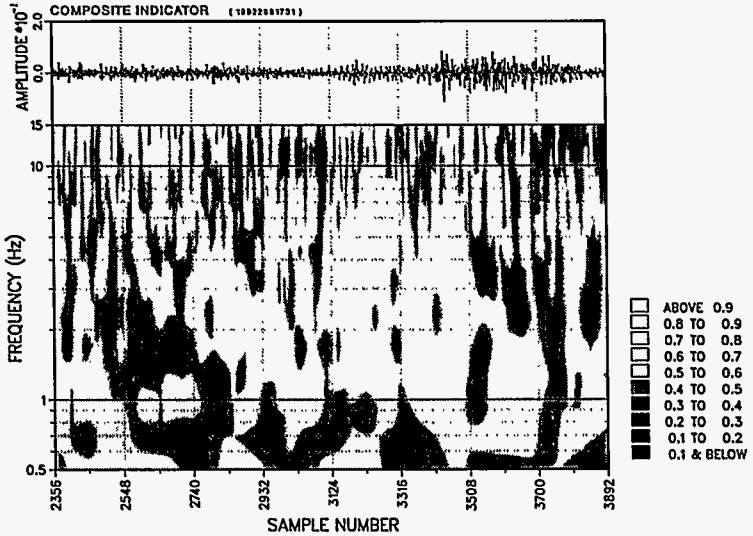

Figure 7a. A Composite Indicator Identifies Windows in Time and Frequency Having Polarized Content For a Quarry Shot

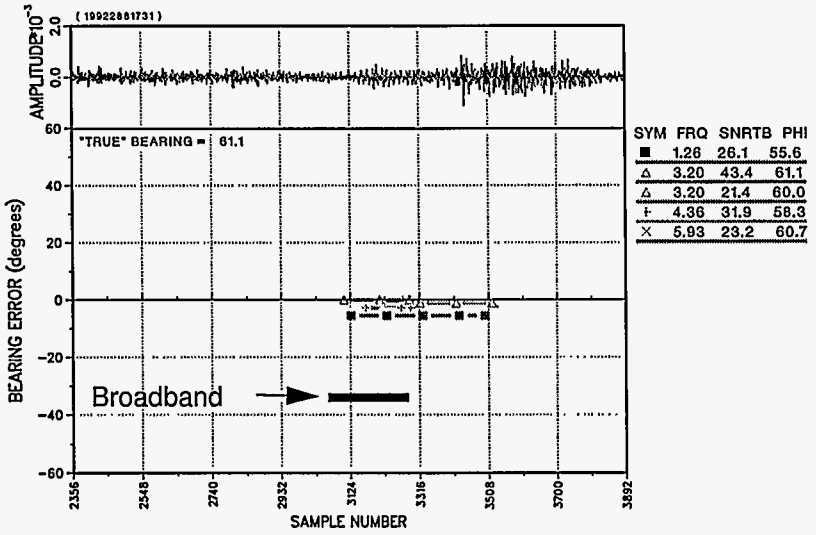

Figure 7b. SEE Estimates on Those WIndows Having 20 or More Effective DOF Produce Reasonably Good Estimates

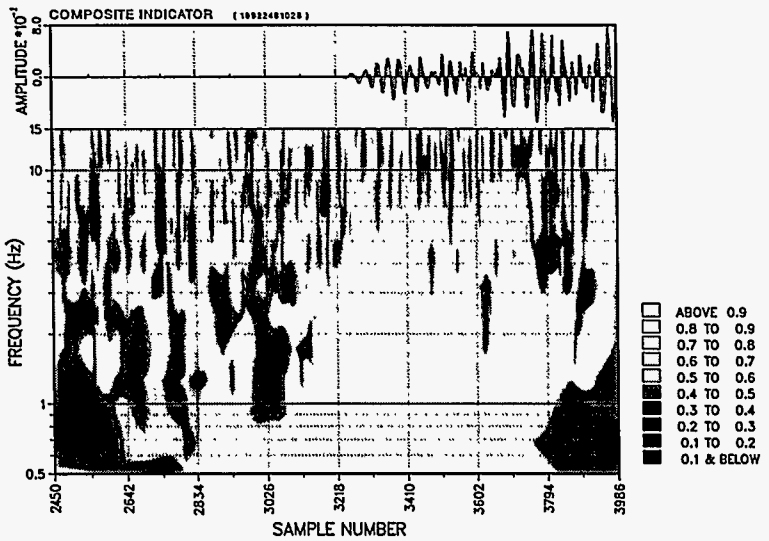

Figure 8a. The Composite Indicator Finds Significant Polarized Content for an Arrival Associated with an Earthquake Occurring in Southern Utah

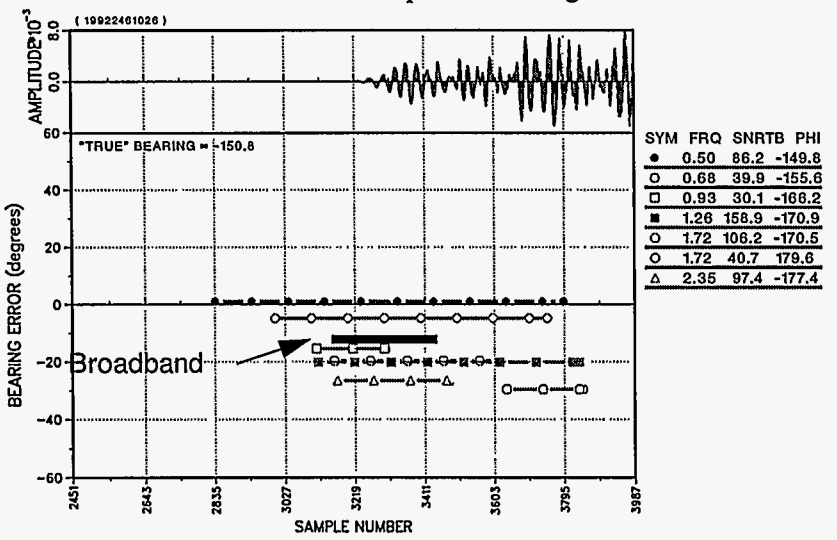

Figure 8b. Strong Evidence for Bearing Dispersion (Frequency Dependent Refraction) Along a Utah to Wyoming Path

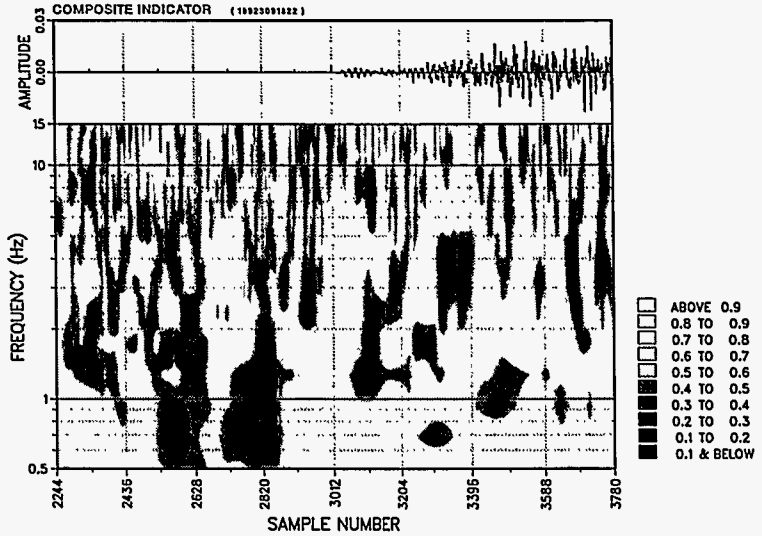

Figure 9a. The Composite Indicator Finds Polarized Content over A Broad Range of Frequencies for an Earthquake in Northern Utah

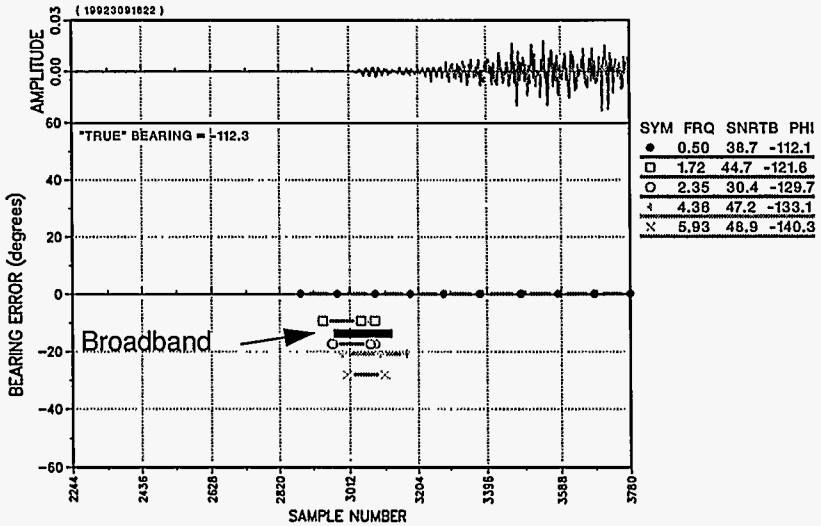

Figure 9b. Additional Evidence for Bearing Dispersion along A Utah to Wyoming Path

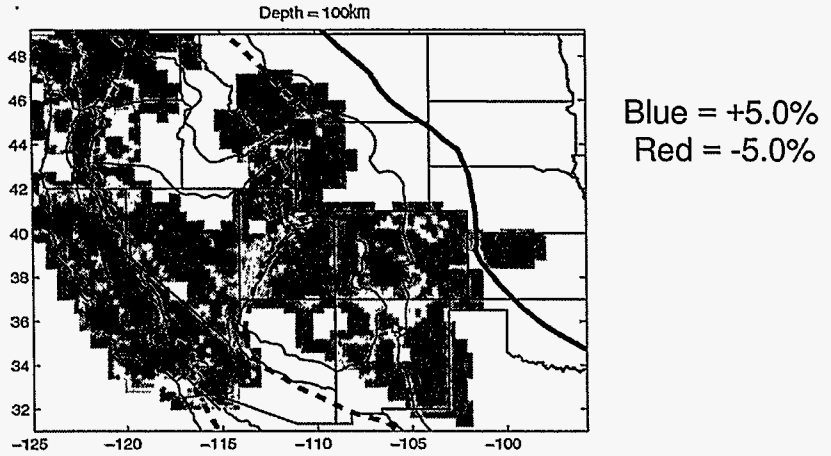

Figure 10. Evidence for Velocity Gradients at a Depth of 100 km Across Western US (Courtesy of K. M. Dueker, University of Colorado)

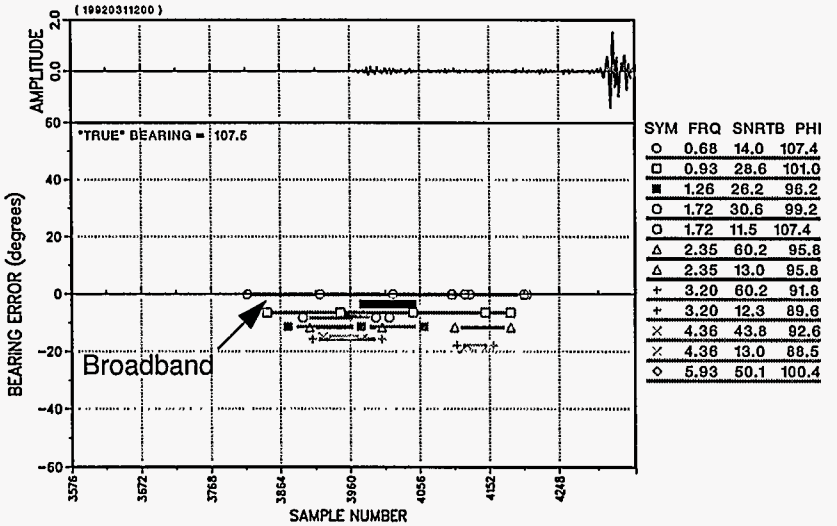

Figure 11. A Complicate Bearing Dispersion Characteristic Can Occur at Local Distances. Dispersion is Evident in Two Arrivals

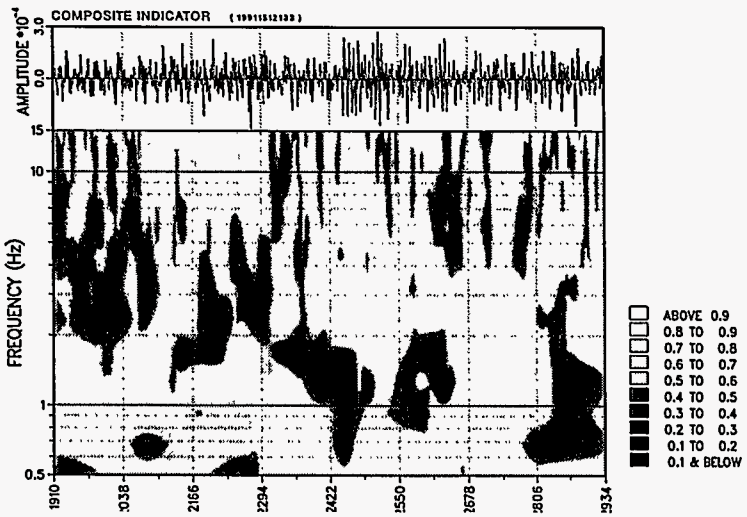

Figure 12a. The Search Process Finds a Strong Polarized Responses Deeper in the P Arrival

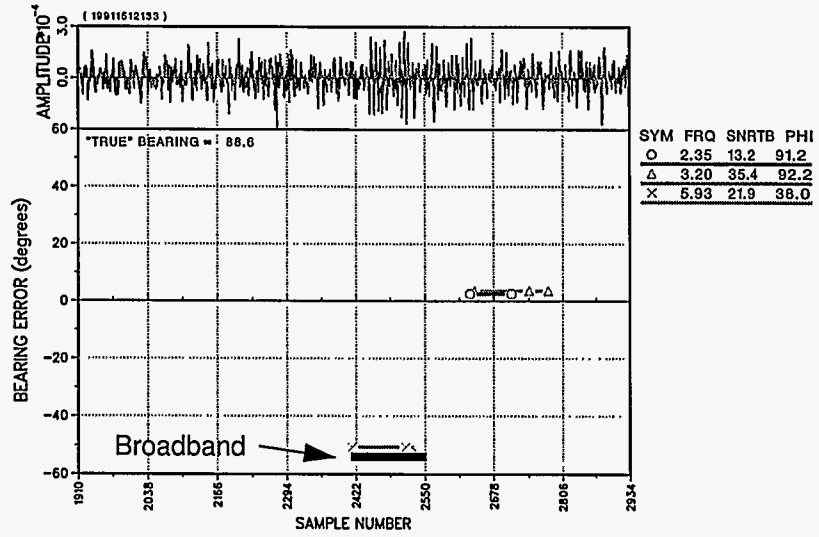

Figure 12b. The Strong Polarized Responses Result in a Pair of Favorable Estimates

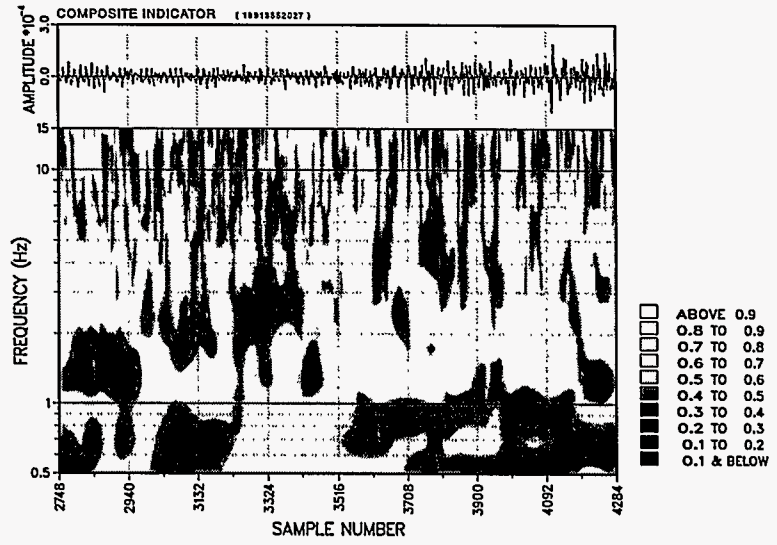

Figure 13a. A Weak and Thin Polarization Response

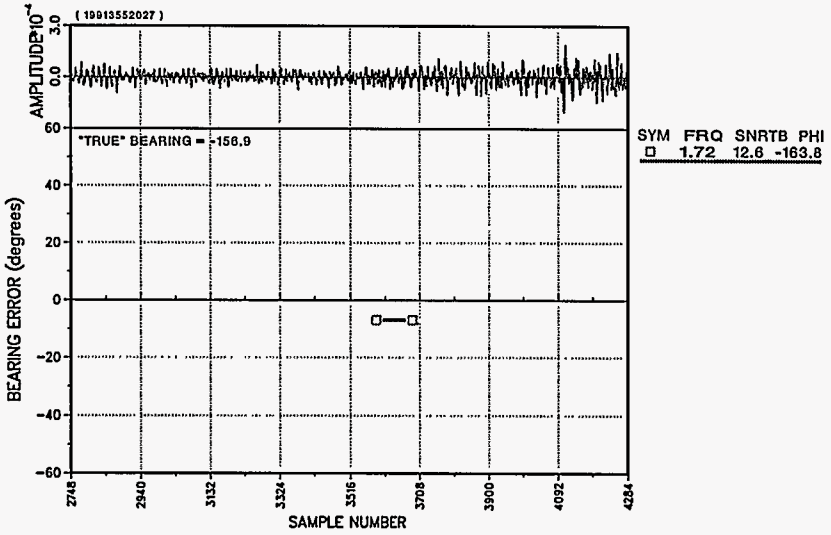

Figure 13b. As a Results of the Poor Polarized Response, Only One Estimate Having but a Few Effective DOF Was Available